

# MECHANISMS OF Pt-Rh THERMOCOUPLE FAILURE BY GASEOUS PHOSPHOROUS IN HIGH TEMPERATURE PROCESSES

Anna Nakano<sup>1,2</sup>, Jinichiro Nakano<sup>1,2</sup>, and James Bennett<sup>1</sup>

<sup>1</sup>U.S. Department of Energy National Energy Technology Laboratory; Albany (OR), USA

<sup>2</sup>AECOM; Albany, OR, USA

## ABSTRACT

Thermocouples are the sensor of choice for monitoring high temperature process. Sensor failure can be caused by a number of reasons related to severe service environments; including slag attack, abrasive wear, shear, protection tube failure, and vapor attack. Depending on the industrial process being monitored, post-mortem analysis of a failed thermocouple assembly to determine causes of failure cannot always be conclusive because process disruption is not always possible. Gasification is one such environment. Coal gasification occurs at temperatures from 1300-1575 °C, with H<sub>2</sub> and CO (syngas) production being used in power or chemical generation. In the severe service environment of a gasifier, thermocouples are placed in protective assemblies that are in contact with refractory liners and the process. Refractory lining shifts or the nature of the process can cause wear, breakage, or failure of the thermocouple protection assembly, allowing the corrosive gas or slag environment to contact thermocouple wires. Corrosive gases in a gasifier originate from the carbon feedstock or the refractory liner, and can contain arsenic, sulfur, phosphorous and other impurities. Current research is investigating the effects of phosphorous gas on the Pt-Rh thermocouple degradation. Gaseous phosphorous interactions with a type B thermocouple were studied non-isothermally by heating samples to 1500 °C, and by heating samples isothermally at 1012 °C in high temperature resistance furnace. CO and CO<sub>2</sub> gases were used to simulate the reducing oxygen partial pressure environment similar to that in an industrial gasifier, and to promote evolution of phosphorus gas. Separately, individual Pt wires with varying Rh contents were tested isothermally in the phosphorous rich reducing environment for different exposure times. The analysis revealed the material degradation was caused by a combination of lowering of the Pt liquidus and by the formation of an intermediate phase at grain boundaries and/or at the gas/solid interfaces. The phosphorous diffusion in the Pt-Rh alloys depended on Rh content. In the low Rh (0, 6, 10 wt.%) alloys, intergranular diffusion was dominant; while intragranular diffusion was governing the P transport in the high Rh alloys (30 wt.%) due to more interactions with Rh. Upon isothermal P exposure, an Rh<sub>2</sub>P intermediate phase formed in all the wires containing Rh, while the pure Pt wire extensively melted at grain boundaries due to phosphorous enrichment within one minute of exposure that led to material degradation. Mechanisms causing thermocouple failure by phosphorous are proposed.

## INTRODUCTION

Pt-Rh alloys are commonly used in high temperature thermocouple sensors for slagging gasification systems. The Rh concentration in a Pt-Rh alloy is typically varied between 0 and 30 wt.% to induce a voltage difference corresponding to the temperature being measured. Examples of commonly used Pt-Rh thermocouples are a type S (consists of pure Pt and Pt-10 wt.% Rh wires); a type R (consists of pure Pt and Pt-13 wt.% Rh wire); and a type B thermocouple (consist of Pt-6 wt.% Rh with Pt-30 wt.% Rh wire) [1]. While Pt is considered to be relatively inert, Pt based thermocouples often suffer failure in severe industrial gasification

environments. An example of the thermocouple sensor readings from the failed gasifier sensor is shown in Fig. 1. Note the sensor underwent severe thermal cycling from high temperatures (up to 1575°C) and high pressure (up to 60 atm), was subject to molten slag attack, and was constantly exposed to corrosive gases. During the gasification process, thermocouple failure can be caused by slag attack, abrasive wear, shear, protection tube failure, and vapor attack by corrosive gases (including As, S, Si and P). Temperature readings are one of the key parameters impacting overall process efficiency. It is therefore essential to understand thermocouple failure mechanisms as a guide to developing future protection strategies.

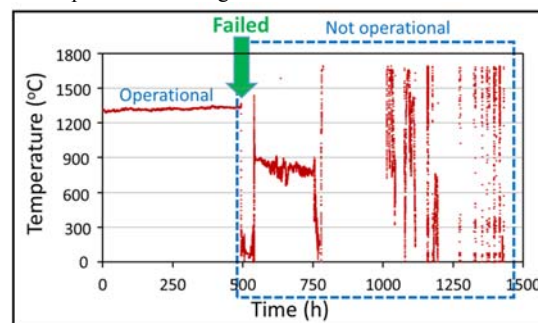


Fig. 1: Thermocouple readings from a commercial gasifier over a two-month time period.

While the impact of As, S, and Si gases on Pt degradation have been well studied, detrimental effects of gaseous P species have not. P may originate from the carbon feedstock or liner materials used in the gasification processes.

In earlier work by the present authors [2], phosphorous movement inside an AlPO<sub>4</sub>-containing gasifier refractory was reported to occur via vapor phase transport, following the breakdown:  $4\text{AlPO}_{4(s)} = 2\text{Al}_2\text{O}_{3(s)} + 2\text{O}_{2(g)} + (\text{P}_2\text{O}_3)_2(g)$ . A similar breakdown is expected for AlP<sub>3</sub>O<sub>9</sub> (metaphosphate):  $\text{AlP}_3\text{O}_9(s) = \text{AlPO}_4(s) + \text{P}_2\text{O}_5(g)$ , where P<sub>2</sub>O<sub>5</sub> gas may be produced instead of (P<sub>2</sub>O<sub>3</sub>)<sub>2</sub> at 700 °C [3]. Decomposition of phosphates producing the gas phases (P<sub>2</sub>O<sub>3</sub>)<sub>2</sub> or P<sub>2</sub>O<sub>5</sub> is impacted by both temperature and oxygen partial pressure; with (P<sub>2</sub>O<sub>3</sub>)<sub>2</sub> or P<sub>2</sub>O<sub>5</sub> increasing with temperature or decreasing with oxygen partial pressure [4]. Phosphorous gas released may interact with the thermocouple installed within the gasifier refractory lining, causing sensor materials failure.

In this study, the effects of phosphorous gas on the Pt-Rh thermocouple degradation was investigated by varying Rh content and exposure times. Gaseous P interactions with a type B thermocouple were analyzed non-isothermally and isothermally in P rich gaseous environments.

## EXPERIMENTAL

The failure of type B thermocouples (94 wt.%Pt-6 wt.% Rh/70 wt.% Pt-30 wt.% Rh) caused by gaseous P species was first analyzed non-isothermally by heating samples to 1500 °C in CO or a mixture of 64 vol.% CO-36 vol.% CO<sub>2</sub>, and then isothermally in CO at 1012 °C in high temperature resistance furnace. Reagent grade aluminum phosphate powder of < 5µm (Alfa Aesar, USA) was used as the source

of gaseous P. It contained about 7.2 wt.% of  $\text{AlP}_3\text{O}_9$ , with the balance being  $\text{AlPO}_4$ . The Pt – 6 wt.% Rh and Pt – 30 wt.% Rh wires of 0.38 mm diameter studied were manufactured by Engelhard (USA) and were oxyacetylene welded at the point where the two wires were joined to make a type B thermocouple. The experimental setup employed in this work is schematically shown in Fig. 2.

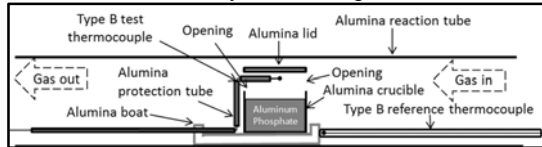


Fig. 2: Schematic experimental set-up employed in this work.

The type B test thermocouple was placed into protection alumina tubing (3 mm ID) with the welded tip exposed to a P-bearing gas above the aluminum phosphate. To generate phosphorous containing gas, two grams of aluminum phosphate powder was placed in a high density alumina crucible (26 mm H  $\times$  22 mm OD  $\times$  18 mm ID) with two openings (4 mm  $\times$  4 mm each) on the gas inlet and outlet sides of the crucible so gas moving through the furnace could pass through the crucible. A high density alumina lid was used to cover the crucible. The type B test thermocouple and the crucible with the aluminum phosphate powder were set on a rectangular alumina boat (450 mm W  $\times$  1050 mm L) within the hot zone of a horizontal CM Rapid Temp 1800 Furnace (USA). The type B reference thermocouple was in a closed alumina protection tube placed next to the alumina boat. A heating rate during experiment was controlled using a programmable temperature controller. Sample temperature changes were continuously recorded by the reference and test thermocouples in-situ via its electromotive force (EMF). To enable isothermal P gas exposure, the thermocouple tip was first heated in 95 vol. %  $\text{N}_2$ -5 vol.%  $\text{O}_2$  to avoid decomposition of aluminum phosphate. At the designated temperature, the furnace gas was switched to CO, releasing P gas by destabilizing the aluminum phosphate. The test thermocouple was quenched in water at room temperature as soon as failure was noted (i.e., EMF output from the sensor assembly discontinued). Immediately after thermocouple failure and prior to quenching, the reaction tube was purged with He at 400 ml/min for 10 min for safety. The experimental procedure leading to thermocouple wire failure was repeated with individual Pt wires containing varying Rh content (100 wt.% Pt, Pt-6 wt.% Rh, Pt-10 wt.% Rh, and Pt-30 wt.% Rh). These wires were quenched after 0 min, 1 min, 3 min, and 5 min of exposure in CO at the desired test temperature. Sample exposure time to P-enriched CO gas was counted from the time when the CO valve was opened in the furnace system. All wires after the test were analyzed for phase changes using scanning electron microscopy with energy dispersive X-ray spectroscopy (SEM-EDS, FEI Inspect F and an Oxford INCA WAVE spectrometer). All the gases used in the experiment were high purity and supplied by Matheson (USA).

## RESULTS AND DISCUSSION

### Non-isothermal test

On heating, thermocouple readings from the experiment conducted in the CO environment indicated failure at 948 °C. In the CO –  $\text{CO}_2$  gas mixture, the discontinuity in EMF signal was noted at 979 °C, which was higher than those in CO. This may be explained by the difference in decomposition temperature and kinetics of aluminum phosphate [4], and subsequent P/Pt-Rh reactions. The decomposition temperature would be lowered with lower

partial pressure of oxygen induced by CO, causing a rapid increase in the vapor pressure of P-bearing gas species above 700 °C [3] on heating, which ultimately led to thermocouple failure at lower temperature. Fig. 3 shows SEM backscattered electron micrographs of cross-sectioned thermocouple samples quenched at failure. In the Pt-6 wt.% Rh wire, P in grain boundaries led to grain boundary melting and the formation of the Pt-Rh compound. The Pt-30 wt.% Rh wires, on the other hand, experienced melting of the outer surfaces dominated by P-containing phases. The presence of the  $(\text{Pt, Rh})_2\text{P}$  phase (dark phase in Fig. 3) is noted in all the quenched thermocouple wires. A greater fraction of the  $(\text{Pt, Rh})_2\text{P}$  phase is observed in the wires treated in the CO gas environment than those treated in the  $\text{CO}/\text{CO}_2$ . Morphology of the  $(\text{Pt, Rh})_2\text{P}$  phase formed in wires with a higher Rh content (30 wt.%) varied depending on radial location, with it being blocky in the outer melted layers and lamellar-like in the lattice near the liquid/Pt-grain interface. The  $(\text{Pt, Rh})_2\text{P}$  phase was only found in the grain boundaries for thermocouple wires with a low Rh content (6 wt.%).

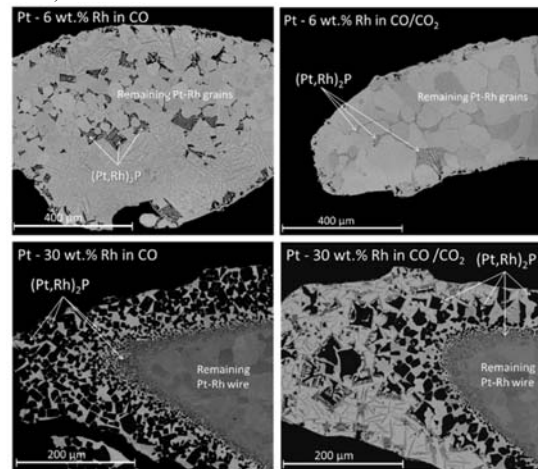


Fig. 3: SEM images of the cross-sectioned thermocouple wires heated in P-enriched environment to 1500 °C and quenched at failure.

### Isothermal test

In order to ensure fast kinetics of the degradation process, a temperature for the isothermal test was chosen to be 1012 °C which is close, but sufficiently higher ( $\approx 60$  °C) than failure temperature noted in the non-isothermal test. Fig. 4-6 shows SEM images of the cross-sectioned Pt-30 wt.% Rh, Pt-6 wt.% Rh and Pt-0 wt.% Rh alloys isothermally exposed to P gas for various times (0 – 5 min) at 1012 °C.

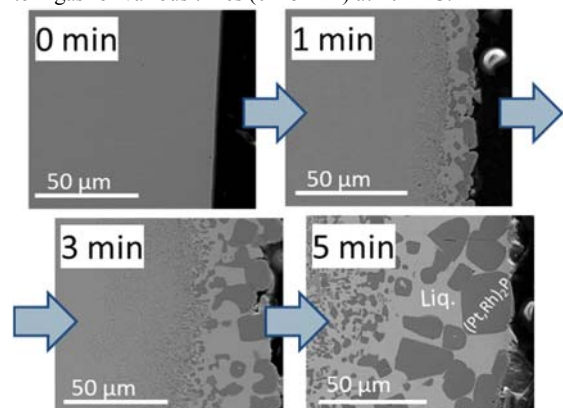


Fig. 4: SEM images of the cross-sectioned Pt-30 wt.% Rh wires quenched after 0 min, 1 min, 3 min, and 5 min of exposure in P-rich CO environment at 1012 °C.

The Pt-10 wt.% Rh showed similar degradation behavior to the Pt-6 wt.% Rh alloy.

A reference alloy without any P exposure (marked as “0 min”) exhibits a smooth outer surface and no apparent damage after similar thermal exposure. For the Pt-30 wt.% Rh alloy with 1 min of isothermal exposure to CO, phosphorous diffused into the grains and interacted with the Pt and Rh, forming the (Pt, Rh)<sub>2</sub>P phase at the gas/ Pt-30 wt.% Rh interface. The Pt-Rh matrix was found melted due to P enrichment. The averaged EDS point analysis of the (Pt, Rh)<sub>2</sub>P phase indicated 33.66 at.% P-57.21 at.% Rh-9.13 at.% Pt. After 3 min of exposure, the phosphorous diffusion progressed deeper into the alloy, thickening the affected zone with larger (Pt, Rh)<sub>2</sub>P precipitates. More Rh from the bulk Pt-Rh wire was consumed in the affected layer. After 5 min of exposure, the Rh<sub>2</sub>P precipitates in the outer layer grew larger, with some reaching 30 μm in size.

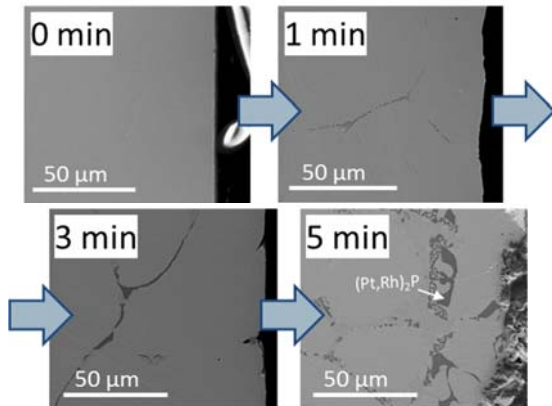


Fig. 5: SEM images of the cross-sectioned Pt-6 wt.% Rh wires quenched after 0 min, 1 min, 3 min, and 5 min of exposure in P-rich CO environment at 1012 °C.

The intergranular diffusion of phosphorous into the Pt-Rh matrix was noted in the Pt-6 wt.% Rh alloy. Rapid P-enrichment in Pt of the grain boundaries facilitated grain boundary melting. One min of exposure to the P-rich atmosphere was long enough to promote the formation of (Pt, Rh)<sub>2</sub>P in the grain boundaries. With longer exposures, more Rh was consumed from the grains, contributing to Rh<sub>2</sub>P growth. EDS analysis indicated the (Pt, Rh)<sub>2</sub>P phase composition to be on average 32.97 at.% P-56.70 at.% Rh-10.32 at.% Pt. The remaining Rh-poor Pt (due to the formation of (Pt, Rh)<sub>2</sub>P) in the grain boundaries was enriched with P, further contributing to melting.

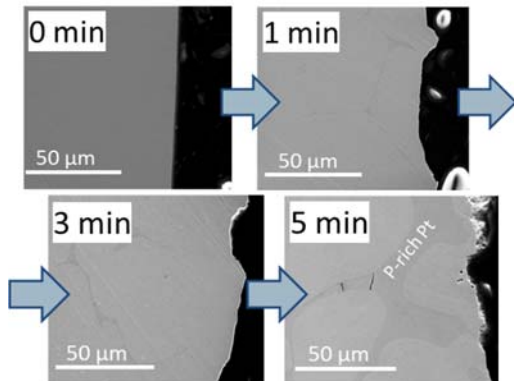


Fig. 6: SEM images of the cross-sectioned Pt-0 wt.% Rh wires quenched after 0 min, 1 min, 3 min, and 5 min of exposure in P-rich CO environment at 1012 °C.

Similar to the Pt-6 wt.% Rh alloy, phosphorous diffused into the Pt-0 wt.% Rh wire along the grains (intergranular diffusion), lowering the melting point of Pt and leading to

grain boundary melting. A much more rapid widening of the grain boundaries was noted in the Pt without Rh (Pt-0 wt.% Rh). After 5 min of P-rich CO gas exposure, structural spalling of the surface grains, or complete melting and flow from the surface would be possible, causing catastrophic damage of the alloy.

The binary P-Rh phase diagram available in the literature [5] indicates possible formation of several P-Rh phases under the experimental conditions evaluated. Those phase: Rh<sub>2</sub>P, Rh<sub>3</sub>P<sub>2</sub>, Rh<sub>4</sub>P<sub>3</sub>, RhP<sub>2</sub> and RhP<sub>3</sub> may form in the P-Rh system, depending on P concentrations. EDS analysis of the alloys exposed to P-enriched CO gas indicated the presence of the Rh<sub>2</sub>P phase (≈ 33 at.% P) with about 10 at.% of Pt present. The Pt and Rh atoms were assumed to be substitutional and share the same crystallographic sites in PRh<sub>2</sub>, as implied by the (Pt + Rh)/P atomic ratio, which is close to that of the Rh<sub>2</sub>P. According to [6], the PtP<sub>2</sub> would form in the P-Pt system only if sufficient P (67 at.%) is present in Pt. PtP<sub>2</sub> was not observed in the alloys under the conditions studied.

### Proposed mechanisms of Pt-Rh alloy failure by P gas

Sensor failure occurs in a P-rich environment can be described by two means: 1) physical failure of the wire due to melting, and/or 2) change in EMF potential of the wire due to wire composition change, leading to false temperature readings.

As temperature rises in the test environment, more P<sub>2</sub>O<sub>5</sub> and/or (P<sub>2</sub>O<sub>3</sub>)<sub>2</sub> gas would be generated through AlP<sub>3</sub>O<sub>9</sub> decomposition in the present atmospheres, according to FactSage 7.0 (FactPS and FToxid databases) calculations, with (P<sub>2</sub>O<sub>3</sub>)<sub>2</sub> being predominant. The formation of the (Pt, Rh)<sub>2</sub>P compound within the sample indicates that dissociation of the P<sub>2</sub>O<sub>5</sub> and/or (P<sub>2</sub>O<sub>3</sub>)<sub>2</sub> gas was necessary to take place at the gas-solid interface for P atoms to diffuse into the Pt-Rh wire.

In the present work, two distinct materials failure mechanisms driven by P diffusion into the Pt-Rh alloys were identified, depending on Rh content. In the Pt alloy with low Rh content (0 – 10 wt.%), intergranular diffusion was dominant, while intragranular diffusion was governing the P mass transport into the Pt alloys with high Rh content (30 wt.%). Each diffusion mechanism created a unique structural degradation, ultimately leading to sensor material failure.

Based on our finding, the two mechanisms of the Pt-Rh alloy degradation by P-bearing gas are proposed here and schematically summarized in Fig. 7:

1. In the first case (low Rh content), material failure is caused primarily by intergranular diffusion of P into the Pt-Rh alloy. P exhibits a higher chemical affinity for Rh to form intermediate phases than for Pt. This is experimentally evidenced by the presence of the P-Rh based intermediate phase while no P-Pt based intermediate phase was observed in samples. With low Rh content, grain boundary diffusion is favored over the lattice diffusion due to insufficient chemical driving force established by local equilibrium at the gas/lattice interface. An Rh concentration drop in the lattice near the grain boundary implies that Rh diffuses from the fcc-Pt lattice to the grain boundaries. At higher temperature, P diffuses more rapidly through grain boundaries where it reacts with Rh to form (Pt, Rh)<sub>2</sub>P. As more P is transported with time, (Pt, Rh)<sub>2</sub>P coalesces and grows in the grain boundaries. The remaining Rh-deficient Pt stays in the surrounding matrix and is continuously fed with incoming P, which locally lowers the liquidus temperature causing the grain boundaries to melt. As a result, the grain

boundaries are widened as more material is consumed from the lattice.

- In the second case (high Rh content), the failure of the Pt–Rh alloy is initiated by intragranular diffusion of P into the lattice. The strong chemical affinity of Rh for P is facilitated through the relatively larger driving force induced by the local equilibrium established at the gas/alloy interface because of the high Rh concentration in the Pt alloy. The majority of P diffuses into the grains and reacts with Rh to form  $(Pt, Rh)_2P$  in the lattice. Further P enrichment facilitates the growth of  $(Pt, Rh)_2P$  and melting of the remaining Rh-poor and P-rich matrix. The size of  $(Pt, Rh)_2P$  is found to be larger toward the gas/metal interface (across the P concentration gradient). As more P diffusion progresses, a local system crosses the original equilibrium tie-line into a 'new' phase region; one where  $(Pt, Rh)_2P$  is in equilibrium with liquid other than with fcc-Pt.

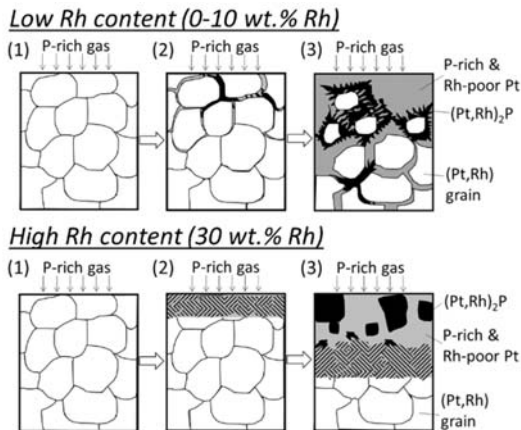


Fig. 7: Proposed mechanisms of Pt-Rh alloy failure by P gas exposure.

In summary, when Pt–Rh alloys in a thermocouple sensor with low Rh content are exposed to P-rich gas: (1) P first migrates into the alloy through grain boundaries; (2) P reacts with Rh (by consuming Rh) from the grains, forming  $(Pt, Rh)_2P$  at grain boundaries; and (3) the remaining P-rich and Rh-poor Pt melts due to further P enrichment, leading to sensor wire failure. When Pt–Rh alloys in a thermocouple sensor with high Rh content are exposed to P-bearing gas: (1) P diffuses directly into the lattice; (2)  $(Pt, Rh)_2P$  forms in the grains as P diffusion proceeds; and finally (3) with further P diffusion, the remaining P-rich and Rh-poor Pt at the P-richer interface with gas liquefies, leading to sensor wire failure.

## CONCLUSIONS

An effect of phosphorous gas generated in slagging gasifier on Pt–Rh thermocouple sensor degradation has been investigated non-isothermally by heating sensors to 1500 °C in CO or 64 vol.% CO–36 vol.% CO<sub>2</sub> and isothermally in CO at 1012 °C. The phosphorous interactions with the Pt–Rh sensor wire alloys depended on Rh content. In the Pt-0 wt.% Rh, Pt-6 wt.% Rh and Pt-10 wt.% Rh alloys, intergranular diffusion was dominant, while intragranular diffusion was governing the P transport into the Pt-30 wt.% Rh alloys. The  $(Pt, Rh)_2P$  phase formed in all wires containing Rh caused wire degradation. The pure Pt wire melted due to phosphorous enrichment, causing wire shape distortion. Overall, the Pt–Rh wires suffered extreme degradation by phosphorous, which led to thermocouple failure. Based on experimental data the mechanisms of

ultimate thermocouple failure by phosphorous was proposed.

## ACKNOWLEDGEMENT

This technical effort was performed in support of the National Energy Technology Laboratory's ongoing research under the RES contract DE-FE0004000. Authors acknowledge Mr. R. Krabbe (NETL) for experimental set-ups, Dr. R. Chinn (NETL) for metallography, Mr. K. Collins (NETL) for SEM-WDS.

## DISCLAIMER

"This report was prepared as an account of work sponsored by an agency of the United States Government. Neither the United States Government nor any agency thereof, nor any of their employees, makes any warranty, express or implied, or assumes any legal liability or responsibility for the accuracy, completeness, or usefulness of any information, apparatus, product, or process disclosed, or represents that its use would not infringe privately owned rights. Reference herein to any specific commercial product, process, or service by trade name, trademark, manufacturer, or otherwise does not necessarily constitute or imply its endorsement, recommendation, or favoring by the United States Government or any agency thereof. The views and opinions of authors expressed herein do not necessarily state or reflect those of the United States Government or any agency thereof."

## REFERENCES

- [1] Park RM. Manual on the Use of Thermocouples in Temperature Measurement sponsored by ASTM Committee E20 on Temperature Measurement, 4th ed. MI; 1993.
- [2] Bennett JP, Kwong K-S, Nakano J, Thomas H, Nakano A. Impact of temperature and oxygen partial pressure on aluminum phosphate in high chrome oxide refractories. *Adv. Sci. Technol.* 2014; 92: 248–257.
- [3] Stone PE, Egan EP, Lehr JR. Phase relationships in the system CaO–Al<sub>2</sub>O<sub>3</sub>–P<sub>2</sub>O<sub>5</sub>. *J. Am. Ceram. Soc.* 1956; 39: 89–98.
- [4] Bennett JP, Riggs B, Nakano A, Nakano J. Causes of phosphate migration in high Cr<sub>2</sub>O<sub>3</sub> gasifier refractories and the impact on slag wear and spalling. *Proceedings of the 14th Biennial Worldwide Congress UNITECR 2015*; 2015 Sep 15-18; Vienna, Austria, 2015.
- [5] Okamoto H. P–Rh (Phosphorus–Rhodium) System. *ASM International. Bulletin. Alloy Phase Diagrams.* 1990; 11: 415-417.
- [6] Okamoto H. P–Pt (Phosphorus–Platinum) System. *ASM International. Bulletin. Alloy Phase Diagrams.* 1990; 11: 511–513.

## Mailing address

Anna Nakano  
 US Department of Energy  
 National Energy Technology Laboratory  
 1450 Queen Ave. S.W.  
 Albany, OR, 97321-2198, U.S.A.